ARTICLES

Electron Transfer-Induced Conformational Changes of Highly Hindered Aromatic Compounds. The Case of Hexakis(alkylsulfonyl)benzenes

Bruno Fabre,* Philippe Hapiot, and Jacques Simonet

Laboratoire d'Electrochimie Moléculaire et Macromoléculaire (Synthèse et Electrosynthèse Organique−Unité Mixte de Recherche no. 6510 associée au CNRS), Université de Rennes 1, Campus de Beaulieu, 35042 Rennes Cedex, France

Received: January 10, 2002; In Final Form: March 19, 2002

The monoelectronic reduction of hexakis(alkylsulfonyl)benzenes (alkyl = methyl **1a**, ethyl **1b**, butyl **1c**, *iso*-propyl **1d**, and *iso*-butyl **1e**) to the corresponding radical anion in dimethylformamide involves two widely separated redox systems, except in the case of **1e** that shows a single perfectly reversible system. Electrochemical data supported by calculations of molecular modeling (DFT and PM3 methods) show the existence of a four-member square scheme for which the neutral and radical anion species can both exist under chair and boat conformations. The relative stability of the conformers was found to be strongly dependent on the nature of the alkyl substituents. Generally, the most stable neutral forms adopt a chairlike geometry, and the radical anions adopt a boatlike geometry. For the most hindered compound **1e**, the steric contribution of the (*iso*-butylsulfonyl) substituents becomes so strong that the conformational changes are considerably slowed, resulting in a frozen chair conformation.

Introduction

The reduction of aromatic sulfones lead to radical anions, for those formation potentials and lifetimes strongly depend on the number and nature of the electron-withdrawing groups bound to the aromatic ring.[1−8] For example, radical anions electrogenerated from mono-,[2] 1,2-bis-,[3,6] and 1,3,5-tris(alkylsulfonyl)-benzenes[4,5] are found to decay along different chemical pathways, namely, bond cleavage, self-radical alkylation and dimerization processes. In contrast, more complex polyaromatic sulfones such as 1,2,4,5-tetrakis-[7] and pentakis(alkylsulfonyl)-benzenes[8] are reversibly reduced, and the electrogenerated radical anions are not degraded within the time scale of the electrochemical experiments. In this class of molecules, the case of some hexakis(alkylsulfonyl)benzenes **1** appears to be very special because the production of the radical anion involves two widely separated redox systems. This electrochemical behavior is highly affected by the nature and bulkiness of the alkyl group bound to the polysulfonyl moiety but also by the temperature and the experimental time. In a preliminary report,[9] it has been proposed that these two redox processes could be related to the existence of two different conformers. Cases of structural modifications induced by a change of the redox state have been reported for several organic molecules.[10−23] However, the observed electrochemical behaviors for the reduction of hexakis-(alkylsulfonyl)benzenes are different as reported cases generally involve either two-electron steps with inversion of potentials[11−13,15,19] or one-electron irreversible steps.[10,13] For the molecules of interest here, the described events are striking and unusual because, depending on the experimental conditions, one or two reversible waves can be observed for a globally one-electron reduction. Among aromatic molecules which undergo structural changes, highly hindered hexasubstituted benzenes[16−22] show conformational flexibility involving some distortions of the aromatic ring. For both steric and electronic reasons, the benzene ring of 1,3,5-tris(dialkylamino)-2,4,6-trinitrobenzene was reported to be severely distorted to a boat form in order to maximize push−pull conjugation.[17] In solution, such a form was seen to inconvert rapidly into a twist conformer by means of a pseudorotation pathway, with an interconversion barrier of 9.1 kcal mol^{-1}. In contrast, the aromatic ring of hexakis(dimethylamino)benzene retains a planar conformation, which is converted into a twist form upon two-electron oxidation to dication.[16,19,20] In connection with these studies, hexakis(trimethylsilyl)benzene[18] and hexakis(trimethylgermyl)benzene[21] were reported to exist as an equilibrium mixture of chair and boat forms. Thus, these representative examples demonstrate that the preference for a specific conformation is directly governed by both the electronic properties and the steric hindrance of the substituents bound to the benzene ring.

In the present paper, the cathodic reduction of these aromatic sulfones is fully investigated in aprotic solvent to determine both the kinetic and thermodynamic constants associated with such phenomena and to analyze them as a function of the alkyl substituent. Also, calculations of molecular modeling based on density functional theory (DFT) and semiempirical methods (PM3) are performed in order to propose an optimized structure for each involved conformer in agreement with electrochemical data.

---

* To whom correspondence should be addressed. Fax: +33 2 23 23 67 32.

10.1021/jp025510p CCC: $22.00

SCHEME 1

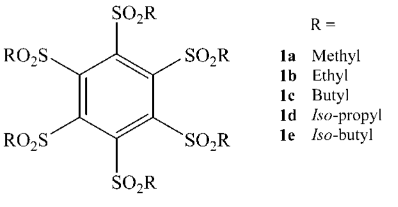

1

Experimental Section

Chemicals. All substrates **1** (see Scheme 1) were prepared according to already reported procedures, consisting in the oxidation of poly(alkylthio)benzenes by *m*-chloroperbenzoic acid.[9,24−27] Dimethylformamide (DMF) from SDS containing less than 50 ppm of water was used without further purification. Tetra-*n*-butylammonium hexafluorophosphate Bu_4NPF_6 was purchased from Fluka (puriss, electrochemical grade).

Instrumentation and Procedures. Linear potential sweep cyclic voltammetry experiments were performed with an Autolab PGSTAT 20 potentiostat from Eco Chemie B. V., equipped with General Purpose Electrochemical System (GPES) software (version 4.5 for Windows). For the highest scan rates, the electrochemical instrumentation consisted of a Tacussel GSTP4 generator and a home-built potentiostat equipped with a positive feedback compensation device,[28] and the data were acquired with a 310 Nicolet oscilloscope. The working electrode was a platinum disk (area: 0.8 mm^2) and the counter electrode was a glassy carbon rod. Potentials were measured against the system Ag/AgI/10^{-1} mol L^{-1} NBu_4I in DMF. Ferrocene was added to the electrolyte solution at the end of each series of experiments. The ferrocene/ferricinium (Fc/Fc^+) couple served as an internal standard, and all reported potentials are referenced to its reversible formal potential. Electrolyte solutions were thoroughly purged and kept under a positive pressure of dry argon during each run. All measurements were carried out at room temperature (20 ± 2 °C). Digital simulations of the voltammograms were performed with the commercial software package DigiSim (Bioanalytical Systems, version 3.03) using the default numerical options with the assumption of planar diffusion. The electron-transfer coefficient, α, was taken as 0.5, and the diffusion coefficients were equal for the all of the species (1×10^{-5} cm^2 s^{-1}). The experimental voltammograms were not subjected to background subtraction.

Theoretical Modeling. The calculations were performed using the Gaussian 98 package[29] for density functional and solvation calculations and the Titan[30] software for semiempirical calculation. Gas-phase geometries and electronic energies were calculated by full optimization without imposed symmetry of the conformations using the B3LYP[31] density functional with the 6-31G* basis set[32,33] or the PM3 semiempirical method.[34] PM3 conformations were validated by frequency calculations. Solvation free energies were calculated on the gas-phase optimized conformations according to the SCRF (self-consistent reaction field) method using the IPCM method[35] and the B3LYP density functional. In this method, the solvent is treated as a continuum of uniform dielectric constant in which the solute is placed into a cavity defined as an isodensity surface of the molecules. The value for the isodensity surface was chosen as 0.001 electrons/$bohr^3$ as used in previous published calculations.[35a]

Results and Discussion

Cyclic Voltammetry of Hexakis(alkylsulfonyl)benzenes Reduction. The electrochemical reduction of hexakis(alkylsulfonyl)benzenes **1** was studied in dimethylformamide (DMF) containing 0.1 mol L^{-1} Bu_4NPF_6 as the supporting electrolyte. The redox behavior was found to be strongly dependent on the nature of the alkyl substituent bound to the sulfone moiety. When the alkyl group was a linear chain (molecules **1a**−**1c**, R = methyl, ethyl, and butyl), their voltammograms displayed one single reduction peak (process A) and one oxidation peak (process B) on the reverse scan. The difference between the two peak potentials was large (around 0.5V). As an example, a typical cyclic voltammogram recorded at a scan rate $v = 0.1$ V s^{-1} is shown in Figure 1A for the sulfone **1b**, R = ethyl ($E^A_{pc} = -0.818$ V and $E^B_{pa} = -0.344$ V vs Fc/Fc^+ where E^A_{pc} and E^B_{pa} are the cathodic and anodic peak potentials for **A** and **B**, respectively). The anodic peak was only observed if the inversion potential was more negative than E^A_{pc} indicating that this process corresponds to the reoxidation of a product formed after reduction of **1b**. Upon increasing the potential scan rate v, E^A_{pc} and E^B_{pa} shift toward negative and positive potentials, respectively. E^A_{pc} and E^B_{pa} were found to vary linearly with log(v) in the range of 0.1−10 V s^{-1}, with slopes of ca. −40 and +36 mV for a 10-fold increase in v (see Figure 2).[36] Within this range of scan rates, the ratios $I^A_{pc}/v^{1/2}$ and $I^B_{pa}/v^{1/2}$ (where I^A_{pc} and I^B_{pa} are the current intensities of the cathodic and anodic peaks) were almost constant indicating diffusion-controlled currents. It is important to notice that after a complete cycle (reduction and oxidation) the initial product is always obtained. It also appears that the shape of the voltammograms and the peak potential values were not significantly modified when the concentration was varied from 0.5 to 5×10^{-3} mol L^{-1}. For scan rates higher than 50 V s^{-1}, a partial reversibility appears for the two systems (Figure 1B) indicating that the chemical reactions following the electron transfers do not interfere at such scan rate. The two formal potentials $E^{\circ\prime}_{A/A^{\bullet-}}$ and $E^{\circ\prime}_{B/B^{\bullet-}}$ were

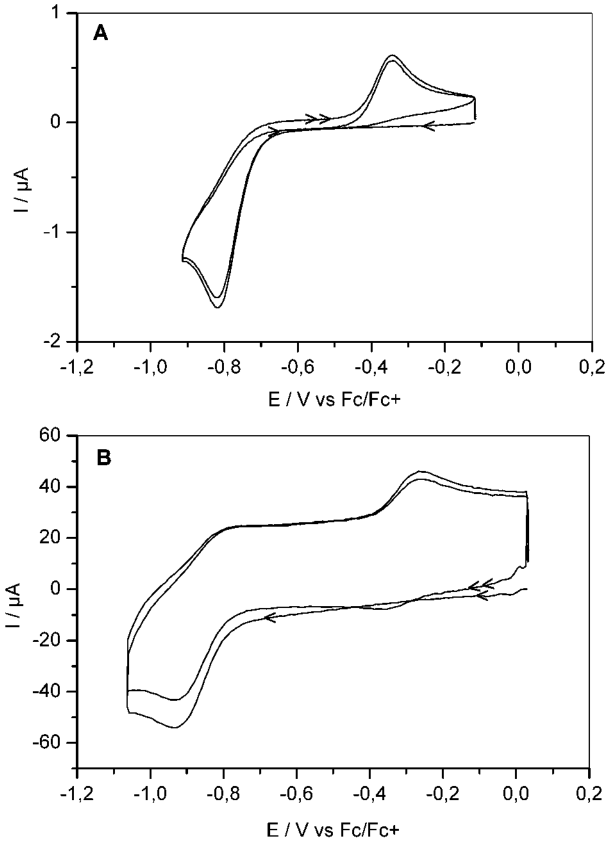

Figure 1. Cyclic voltammograms of **1b** (1×10^{-3} mol L^{-1}) in DMF + 10^{-1} mol L^{-1} Bu_4NPF_6 at 0.1 (A) and 100 V s^{-1} (B).

TABLE 1: Simulation Data of the Cathodic Reduction of Different Hexakis(alkylsulfonyl)benzenes in DMF + 10^{-1} mol L^{-1} Bu_4NPF_6 on Pt Electrode (Temperature 298 K)

	$E^{\circ\prime}_{A/A^{\bullet-}}$/ V[a]	$E^{\circ\prime}_{B/B^{\bullet-}}$/ V[a]	$k_{s,A}$/ cm s^{-1}[b]	$k_{s,B}$/ cm s^{-1}[b]	$K_{B^{\bullet-}/A^{\bullet-}}$[c]	$k_{A^{\bullet-}\rightarrow B^{\bullet-}}$/ s^{-1}	$K_{B/A}$[d]	$k_{B\rightarrow A}$/ s^{-1}
1a	−0.777	−0.280	0.20	0.20	$1.0 \times 10^3 - 1.0 \times 10^5$	150	$6 \times 10^{-6} - 6 \times 10^{-4}$	150
1b	−0.858	−0.302	0.10	0.20	$1.0 \times 10^3 - 1.0 \times 10^6$	1500	$4 \times 10^{-7} - 4 \times 10^{-4}$	200
1c	−0.943	−0.293	0.02	0.02	5.0×10^7	>1000	1.1×10^{-3}	200
1d	−0.635	−0.290	0.04	0.04	3.0×10^4	300	4.6×10^{-2}	300
1e[e]	−0.601		0.04			<0.005		

[a] Vs Fc/Fc+. [b] Uncorrected for double-layer effects. [c] $K_{B^{\bullet-}/A^{\bullet-}} = [\mathbf{B}^{\bullet-}]_{eq}/[\mathbf{A}^{\bullet-}]_{eq} = k_{A^{\bullet-}\rightarrow B^{\bullet-}}/k_{B^{\bullet-}\rightarrow A^{\bullet-}}$. [d] $K_{B/A} = [\mathbf{B}]_{eq}/[\mathbf{A}]_{eq} = k_{A\rightarrow B}/k_{B\rightarrow A}$. [e] A single one-electron reversible system was observed for this compound, at all used scan rates.

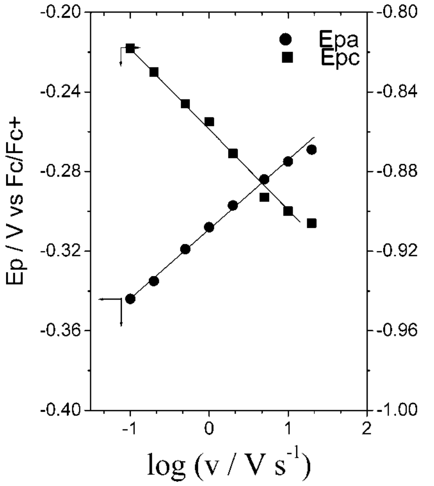

Figure 2. E^{B}_{pa} and E^{A}_{pc} − log v plots for the reduction of **1b** (1×10^{-3} mol L^{-1}) in DMF + 10^{-1} mol L^{-1} Bu_4NPF_6.

derived as the half-sum between the two corresponding peak potentials (we note $\mathbf{A}/\mathbf{A}^{\bullet-}$ and $\mathbf{B}/\mathbf{B}^{\bullet-}$ the couples with the most and least negative potentials respectively). The peak-to-peak separations for each system ΔE^{A}_{p} and ΔE^{B}_{p} were larger than the 56 mV expected for a Nernstian one-electron charge transfer indicating a kinetics limitation by the heterogeneous electron transfers. The corresponding apparent heterogeneous electron-transfer standard rate constants (uncorrected from the double layer effect) $k_{s,A}$ and $k_{s,B}$ were derived from ΔE^{A}_{p} and ΔE^{B}_{p}, respectively.[37,38]

Concerning the two other linear alkyl chain-substituted derivatives **1a** and **1c**, their voltammograms display comparable patterns with similar variations of the characteristic parameters (E^{A}_{pc}, E^{B}_{pa}, $I^{A}_{pc}/v^{1/2}$, and $I^{B}_{pa}/v^{1/2}$) with v (similar to Figure 2). The only noticeable differences were the values of $E^{\circ\prime}$ and ΔE_p determined at the highest scan rates (see Table 1). Without presuming of the nature of the chemical step, all of these observations can be rationalized in terms of a four-member scheme (Scheme 2)

SCHEME 2: Square Scheme Depicting the Different Species Involved in the Reduction of Hexakis(alkylsulfonyl)benzenes

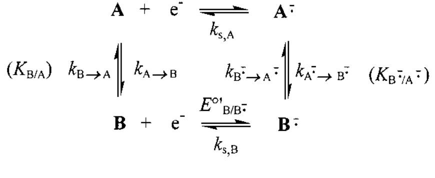

involving two EC mechanisms (EC: one-electron electrochemical step followed by a first-order chemical reaction).[39] In other words, the radical anion electrogenerated at E^{A}_{pc} is rapidly converted into another species which is subsequently oxidized at the much more positive potential E^{B}_{pa}. Similarly, the neutral form produced at E^{B}_{pa} is converted to a more difficult reducible species. To extract the chemical kinetics rate constants, it is interesting to note that the global mechanistic scheme can be simplified into two independent EC processes in the case where **B** is more easily reduced than **A** ($E^{\circ\prime}_{B/B^{\bullet-}} > E^{\circ\prime}_{A/A^{\bullet-}}$) and provided that the chemical steps are irreversible.[14,40] For the reductions of **1a** and **1b**, this condition is confirmed by the absence of a cathodic peak around −0.3 V in the first sweep whatever the scan rate, which indicates that the starting concentration of **B** is negligible, i.e., $K_{B/A} = [\mathbf{B}]_{eq}/[\mathbf{A}]_{eq} \ll 1$ and that the rate constant $k_{A\rightarrow B}$ is too low to produce **B** during the experimental time. In such case, the two kinetics constants $k_{A^{\bullet-}\rightarrow B^{\bullet-}}$ and $k_{B\rightarrow A}$, (corresponding to the conversion of $\mathbf{A}^{\bullet-}$ to $\mathbf{B}^{\bullet-}$ and **B** to **A**, respectively) are directly measured from the scan rates for which the voltammograms become reversible (see Table 1).[37,38]

Using the determined values of $E^{\circ\prime}$, k, and k_s, the voltammograms were compared with simulated curves at different scan rates to extract the other parameters. For all of the investigated hexasulfones, good agreements were found between the experimental and simulated voltammograms in a large range scan rates from 0.1 to 100 V s^{-1} (Figure 3) justifying the assumption of a four-member scheme mechanism. For **1a** and **1b**, the simulations allow the estimation of a range for the two equilibrium constants $K_{B^{\bullet-}/A^{\bullet-}}$ and $K_{B/A}$ that should be compatible with the irreversible chemical reaction steps (for **1b**: $1.0 \times 10^3 < K_{B^{\bullet-}/A^{\bullet-}} < 1.0 \times 10^6$ and $4 \times 10^{-7} < K_{B/A} < 4 \times 10^{-4}$).[41] In contrast with the linear alkyl chain-substituted derivatives, the voltammograms recorded for **1d** (R = *iso*-propyl) differ markedly (Figure 4A). First, for low scan rates (0.05−0.2 V s^{-1}), **1d** exhibits a reversible system at −0.350 V followed by an irreversible cathodic peak. Upon increasing the scan rate, the first cathodic peak is replaced by a plateau, whereas the shape of the related anodic peak remains unchanged. Furthermore, the ratio between the anodic peak and cathodic plateau currents became larger than 1.0 and increased with v. This behavior indicates a change in the kinetics control and that the chemical step **A** → **B** acts now as a preequilibrium prior to the electron transfer.[42,43] Adjustment of the experimental voltammograms with the simulated curves gives us a measure of $K_{B/A} = 4.6 \times 10^{-2}$ and $K_{B^{\bullet-}/A^{\bullet-}} = 3 \times 10^4$ (Figure 4), which reveals that the most stable form at the radical anion level is $\mathbf{B}^{\bullet-}$. For **1c**, a small plateau was also observed during the first scan recorded at the lowest scan rate (0.05−0.1 V s^{-1}) corresponding to a similar CE kinetics situation but with a lower equilibrium constant $K_{B/A}$. For **1e** (R = *iso*-butyl), only one reversible system was observed whatever the scan rate. The measured $E^{\circ\prime}$ was similar to the other molecules and corresponds to the A system. The most likely interpretation of this behavior in terms of the previous square scheme mechanism is that the chemical reactions involved in the conversion of **A** to **B** do not occur at

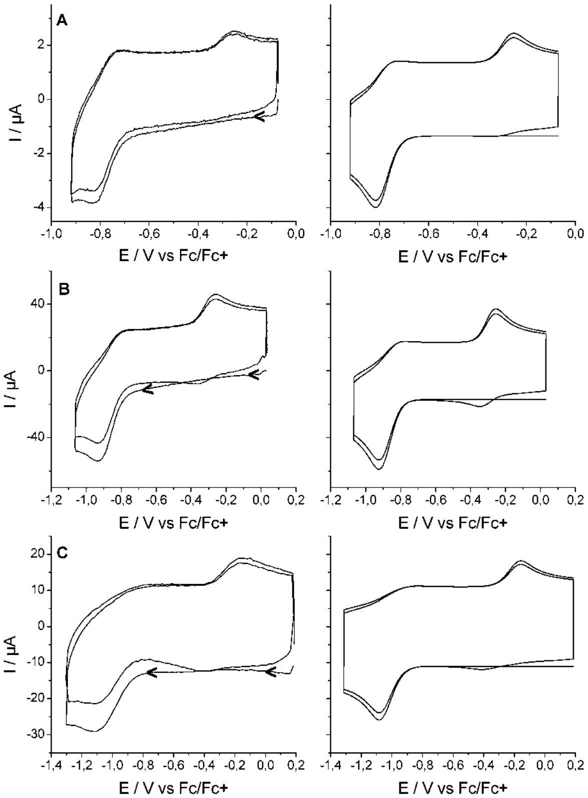

Figure 3. Experimental (left) and simulated (right) cyclic voltammograms of 0.35×10^{-3} mol L^{-1} **1a** at 10 V s^{-1} (A), 1×10^{-3} mol L^{-1} **1b** at 100 V s^{-1} (B), and 0.75×10^{-3} mol L^{-1} **1c** at 100 V s^{-1} (C). Double-layer capacitance C_d values were introduced into the simulation: 1.35×10^{-4} (A), 3×10^{-5} (B), and 5×10^{-5} F cm^{-2} (C). The other simulation parameters are indicated in Table 1.

time scale of the voltammetric experiment resulting in the observation of the sole system **A**.

Molecular Modeling of Hexakis(alkylsulfonyl)benzenes. The previous kinetics investigations allow us to establish that all of the studied hexasulfones follow the same general square scheme mechanism. The next question concerns the nature of the chemical reaction involved in the transformation of **A** to **B**. As we suggested previously, a possible explanation for the square scheme mechanism is related to the existence of two conformers for both the neutral species and the radical anions. To investigate this hypothesis, we performed a series of molecular modeling calculations to determine both the geometries and the stabilities of the neutral and radical anion species. To minimize the size of the molecules and thus calculation times, we focused on the methyl substituted compound **1a**. The geometry optimizations were performed with the semiempirical PM3 method and with the density functional B3LYP using the 6-31G* basis set. For neutral **1a**, the conformer with the lowest energy displays a “chair” like geometry (Figure 5). This prediction was in good agreement with X-ray diffraction structure determinations of bulky hexasulfones (R = *n*-butyl) for which chair conformer was already found for the neutral molecule.[9] In the experimental structure and in those obtained from the PM3 and DFT calculations, the benzene is distorted and the six SO_2 groups are located alternately up and down from the plane of the aromatic ring.

The optimized geometry calculated for $\mathbf{1a}^{\bullet-}$ was very different from that of **1a**. The most stable radical anion now adopts a “boat” conformer with a C_s symmetry where alkylsulfonyl substituents S1 and S4 are nonequivalent.[44] In the absence of crystallographic data for the radical anion species, EPR data

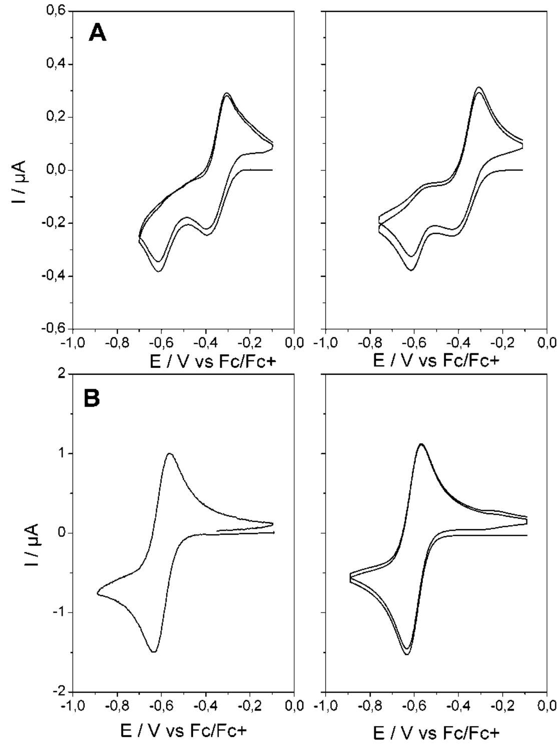

Figure 4. Experimental (left) and simulated (right) cyclic voltammograms of 0.75×10^{-3} mol L^{-1} **1d** (A) and 1×10^{-3} mol L^{-1} **1e** (B) at 0.1 V s^{-1}. $C_d = 5 \times 10^{-5}$ F cm^{-2}. The other simulation parameters are indicated in Table 1.

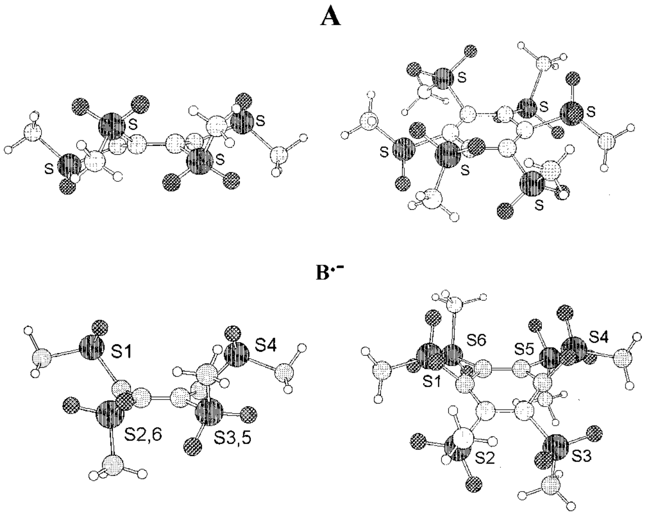

Figure 5. Optimized geometries calculated at the B3LYP/6-31G* level, of the neutral **A** and radical anion $\mathbf{B}^{\bullet-}$ conformers of **1a**. Side view (left) and top view (right). See text for atoms numbers on $\mathbf{B}^{\bullet-}$.

reported in our previous report[9] provide additional evidence for the boat form. Indeed, a 1:2:1 triplet was observed at room temperature for the radical anion electrogenerated from **1b** or **1c** indicating that one CH_2 group bound to one sulfone moiety was nonequivalent to the five others as in agreement with our calculated geometry.[45] Such a result precludes a planar benzene ring as a more complex EPR spectrum having theoretically 13 lines would be expected in the case where all of the six (alkylsulfonyl) substituents were equivalent. A geometry of the radical anion with a structure similar to the neutral form (chair) and, inversely, a geometry of neutral with a structure similar to the radical anion (boat) were also obtained, but their respective energies were higher. Similar types of conformers were obtained

TABLE 2: Molecular Modeling of 1a and 1a$^{\bullet -}$ [a]

	ΔU_{el} or $\Delta(\Delta H_{\mathrm{f}})$/kJ mol$^{-1\,b}$		
method	neutral	radical anion	$\Delta E°$/V^{c}
PM3	24.3	−13.4	0.39
B3LYP/6-31G*//B3LYP/6-31G*	59.4	−16.7	0.79
B3LYP/6-31+G*//B3LYP/6-31G*	58.6	−18.4	0.80
B3LYP/6-31G*//B3LYP/6-31G*, IPCM ($\epsilon = 36.64$)	41.4	−37.2	0.82
experimental[d]	18.4−29.3	−28.5 to −17.2	0.50

[a] Estimations of the thermodynamic stabilities of boat versus chair conformers. [b] For DFT calculations, $\Delta U_{\mathrm{el}} = (U_{\mathrm{el,boat}} - U_{\mathrm{el,chair}})$, and for PM3, $\Delta(\Delta H_{\mathrm{f}}) = (\Delta H_{\mathrm{f,boat}} - \Delta H_{\mathrm{f,chair}})$. [c] $\Delta E° = E°_{\mathrm{boat}} - E°_{\mathrm{chair}}$ with $\Delta E° \approx -1/F[(U_{\mathrm{el,radical\ anion}} - U_{\mathrm{el,neutral}})_{\mathrm{boat}} - (U_{\mathrm{el,radical\ anion}} - U_{\mathrm{el,neutral}})_{\mathrm{chair}}]$ for DFT, and $\Delta E° \approx -1/F[(\Delta H_{\mathrm{f,radical\ anion}} - \Delta H_{\mathrm{f,neutral}})_{\mathrm{boat}} - (\Delta H_{\mathrm{f,radical\ anion}} - \Delta H_{\mathrm{f,neutral}})_{\mathrm{chair}}]$ for PM3. [d] The energetic values are calculated from the equilibrium constants $K_{\mathrm{B/A}}$ and $K_{\mathrm{B^{\bullet -}/A^{\bullet -}}}$ given in Table 1. Also, it is assumed that the standard potential $E°$ is equivalent to the formal potential $E°'$.

TABLE 3: Comparison between Experimental and PM3 Theoretical Energies Calculations

	$\Delta E°$/V		$K_{\mathrm{B/A}}$		$K_{\mathrm{B^{\bullet -}/A^{\bullet -}}}$	
compd	exp	theo[a]	exp	theo[b]	exp	theo[b]
1a	0.50	0.39	$6 \times 10^{-6} - 6 \times 10^{-4}$	5×10^{-5}	$10^{3} - 10^{5}$	2×10^{2}
1b	0.56	0.41	$4 \times 10^{-7} - 4 \times 10^{-4}$	2×10^{-6}	$10^{3} - 10^{6}$	2×10^{2}
1c	0.65	0.50	1.1×10^{-3}	3×10^{-6}	5.0×10^{7}	10^{3}

[a] $\Delta E° = E°_{\mathrm{boat}} - E°_{\mathrm{chair}}$ with $\Delta E° \approx -1/F\ [(\Delta H_{\mathrm{f,radical\ anion}} - \Delta H_{\mathrm{f,neutral}})_{\mathrm{boat}} - (\Delta H_{\mathrm{f,radical\ anion}} - \Delta H_{\mathrm{f,neutral}})_{\mathrm{chair}}]$. [b] Determined from $\Delta(\Delta H_{\mathrm{f}})$ given in Table 2.

both by PM3 and B3LYP/6-31G*, and PM3 geometries were validated as corresponding to true energy minima by frequency calculations confirming that **1a** and **1a**$^{\bullet -}$ both exist under boat and chair conformers. The relative stabilities of the boat conformer versus the chair conformer and equilibrium constants for **1a** and **1a**$^{\bullet -}$ can be estimated from the differences between their heats of formation ΔH_{f} for PM3 (or their electronic energy U_{el} for DFT) calculated in gas phase. Similarly, the standard potential differences $\Delta E° = E°_{\mathrm{boat}} - E°_{\mathrm{chair}}$ for the two couples can also be estimated from the differences between their individual ΔH_{f} (or their electronic energy U_{el} for DFT; Table 2).

To check the validity of the method, we investigated the effects of the basis set and solvation on our thermodynamic estimations. The second effect may be considerable as all of the calculations concern molecules in gas phase. The introduction of diffuse functions in the basis set modifies the individual electronic energies but has little effect on the calculated differences. Solvation energies in DMF ($\epsilon = 36.64$) were estimated by means of the IPCM method (see experimental part). As expected, solvation decreases considerably the energies of the radical anions, but it is noticeable that stabilization is larger for the boat conformers than for the chair ones certainly because of higher charge localization in the boat conformer. However, the difference $\Delta E°$ was not considerably modified by solvation. Thus, the use of the PM3 methodology seems justified to predict experimental trends for the other members of the series (**1b** and **1c**) taking into account in the discussion of the experimental data, that solvation will favor the boat conformers.[46]

As seen in Table 3, both experimental data and theoretical calculations show an inversion for the conformers stabilities when passing from the neutral to the radical anion. For the neutral sulfones **1a**−**c**, a chair form is predicted to be the most stable conformer in agreement with the experimental observations and the measured equilibrium constants. On the contrary, the boat conformer becomes the most stable conformer for the radical anion. The calculations also predict that the boat conformers are easier to reduce by about 0.4−0.5 V in agreement with the experimental observations. All of these results are consistent with the proposed square scheme mechanism where **A** and **B** represent the chair and boat conformers, respectively. It is noticeable that the geometries of the two conformers are very different and consequently that considerable conformational changes are associated with the electron transfer. However, the electron transfer and the conformation changes occur in two discrete steps, the reduction of A leads to a transient radical anion that is rapidly converted to the other conformer as attested by the observed instability of both **A**$^{\bullet -}$ and **B**. The large amplitude of these modifications which involves changes in the bond lengths and angles implies large reorganization energies. These points are confirmed by the rather modest kinetic rate constants measured for the structural changes that remain in the 10^{3} s^{-1} and also explain that both types of conformers (boat and chair) are easily observed.

Concerning the substituent effects, it is verified that the steric hindrance increases with the number of the carbon atoms in the alkyl chain and the branching on the α-carbon atom. However, it remains difficult to obtain a general rule as the steric hindrance of the alkyl group affects the four species involved in the square scheme. In all cases, it is noticeable that a good agreement is obtained between the experimental $\Delta E°'$ variation and the calculation when changing the size of the substituent. As an overall trend for the experimental data (see Table 1), the stability of the boat conformer increases for the neutral sulfone with the bulkiness of the substituent. This effect on $E°'_{\mathrm{A/A^{\bullet -}}}$ and $E°'_{\mathrm{B/B^{\bullet -}}}$ is also difficult to rationalize. $E°'_{\mathrm{A/A^{\bullet -}}}$ decreases weakly from **1a** to **1c** but increases dramatically for **1d**, whereas $E°'_{\mathrm{B/B^{\bullet -}}}$ is almost unchanged (Table 1). Intuitively, it is conceivable that the boat conformer is less sensitive to substituent effects than the chair form owing to smaller steric constraints caused by the alkylsulfonyl groups. The fact that the reduction of the chair is a more difficult form when going from **1a** to **1c** can be explained by increasing steric interactions of the linear alkyl chains. Following this line, the reduction potential of chair **1d** should be more negative than that of **1c**. Experimentally, the contrary situation is encountered, as the chair form of **1d** possesses the least negative reduction potential, which is consistent with a better stabilization of the radical anion or destabilization of the neutral species of **1d** for the chair form. Because the geometry optimization of **1d** has not been achieved, it remains difficult to discuss about potential structural differences between its chair conformer and that of **1a**−**c**. However, it appears that the optimized chair conformers of **1a**−**c** are not significantly deformed when the size of the substituents is changed if one refers to the dihedral folding angles of the aromatic ring passing from 14.8° (average) at the neutral state to 19.1° at the radical anion state. Finally, besides the steric effects, the electronic contribution of the substituents cannot be involved to account for the large observed differences between **1d** and **1a**−**c** as the electron donating contributions are not expected to change much between the different alkylsulfonyl groups.[47] In the case of the most hindered compound **1e**, the steric contribution of the (*iso*-butylsulfonyl) substituents becomes so strong that the conformational changes are considerably slowed. As a result, the voltammetric reduction of this compound shows a single reversible system indicating that the conformer is frozen in the chair conformation as the energy barrier for the structural changes becomes too high. Concerning the electron-transfer rates, the global analysis of data in Table

1 indicates that the value of k_s determined for each redox conformer decreases from 0.2 to 0.02−0.04 cm s^{-1} as the size of the alkyl group increases. This effect reflects a larger distance between the redox sites and the electrode during the electron-transfer resulting in a decrease of the apparent standard rate constant uncorrected from the double layer effects.[48]

Conclusion

The unusual behavior observed for the one-electron reduction of hexakis(alkylsulfonyl)benzenes can be explained by the existence of two conformers that are easily interconverted through single electron-transfer. If conformational changes have been reported in several instances in electrochemical investigation, they are generally associated with multielectronic reduction. In that sense, the reduction of these substituted sulfones that are chemically reversible and involve only one-electron reduction appears to be special. An essential feature of this study is the control of the structural changes of the benzene ring through the steric hindrance of the alkyl substituents. So, various situations can occur depending on both kinetics and thermodynamics of the conformational interconversion between the chair and boat forms. Linear alkyl chain-substituted derivatives (namely, **1a**−**c**) are stable under their chair forms, whereas their respective radical anions adopt a boatlike geometry. The coexistence of the two conformers is observed at the neutral state for hexakis(*iso*-propylsulfonyl)benzene **1d**, whereas the most hindered *iso*-butylsulfonyl-substituted compound **1e** is locked in a chair form. Such a conformational versatility within a same class of aromatic compounds is an interesting possibility for the design of molecules in which large conformational modification can be triggered by a single electron transfer. Through a fine-tuning of the length and the steric hindrance of the alkyl group, it seems possible to control the relative stabilities of the different redox species. Work is currently under investigation in order to prepare other redox-active highly hindered molecules in which steric factors can lock in or create a strong preference for a specific conformation.

Acknowledgment. The authors are indebted to Drs. E. Furet and R. Gauthier (ENSCR, Rennes) for their help in preliminary works concerning the molecular modelization of the sulfones (semiempirical calculations of the chair isomers). The authors also thank Dr. A. Ghanimi for the synthesis of some of the substituted sulfones.

Supporting Information Available: Stereoviews of the optimized chair and boat conformers determined from the DFT B3LYP/6-31G* (only for **1a**) and semiempirical PM3 (**1a**, **1b** and **1c**) methods with the corresponding Cartesian coordinates and energies (33 pages). This material is available free of charge via the Internet at http://pubs.acs.org.

References and Notes

(1) Simonet, J. In *The Chemistry of Sulfones and Sulphoxides*; Pataï, S., Rappoport, Z., Stirling, C. J. M., Eds.; Wiley & Sons: New York, 1988; p 1001.

(2) Mabon, G.; Chaquid El Badre, M.; Simonet, J. *Bull. Soc. Chim. Fr.* **1992**, *129*, 9.

(3) Belkasmioui, A.; Simonet, J. *Tetrahedron Lett.* **1991**, *32*, 2481.

(4) Benaskar, M.; Simonet, J. *Tetrahedron Lett.* **1994**, *35*, 1727.

(5) Simonet, J.; Lund, H. *Acta Chem. Scand., Ser. B* **1977**, *37*, 909.

(6) Cauliez, P.; Benaskar, M.; Simonet, J. *Electrochim. Acta* **1997**, *42*, 2199.

(7) Simonet, J. In *The Chemistry of sulphur-containing functional groups*; Pataï, S., Rappoport, Z., Eds.; Wiley & Sons: New York, 1993; p 439.

(8) Ghanimi, A.; Simonet, J. *J. Electroanal. Chem.* **1997**, *425*, 217.

(9) Ghanimi, A.; Fabre, B.; Simonet, J. *New J. Chem.* **1998**, *831*.

(10) Brielbeck, B.; Rühl, J. C.; Evans, D. H. *J. Am. Chem. Soc.* **1993**, *115*, 11898.

(11) Hu, K.; Evans, D. H. *J. Phys. Chem.* **1996**, *100*, 3030.

(12) Hu, K.; Evans, D. H. *J. Electroanal. Chem.* **1997**, *423*, 29.

(13) (a) Nielsen, S. F. *Acc. Chem. Res.* **1981**, *14*, 131. (b) Evans, D. H.; O'Connell, K. M. Conformational Change and Isomerization Associated with Electrode Reactions. In *Electroanalytical Chemistry, A Series of Advances*; Bard, A. J., Ed.; Marcel Dekker: New York, 1986; Vol. 14, pp 113−207.

(14) Evans, D. H. *Chem. Rev.* **1990**, *90*, 739 and references therein.

(15) Bellec, N.; Boubekeur, K.; Carlier, R.; Hapiot, P.; Lorcy, D.; Tallec, A. *J. Phys. Chem. A* **2000**, *104*, 9750.

(16) Chance, J. M.; Kahr, B.; Buda, A. B.; Toscano, J. P.; Mislow, K. *J. Org. Chem.* **1988**, *53*, 3226.

(17) Chance, J. M.; Kahr, B.; Buda, A. B.; Siegel, J. S. *J. Am. Chem. Soc.* **1989**, *111*, 5940.

(18) Sakurai, H.; Ebata, K.; Kabuto, C.; Sekiguchi, A. *J. Am. Chem. Soc.* **1990**, *112*, 1799.

(19) Speiser, B.; Würde, M.; Maichle-Mössmer, C. *Chem. Eur. J.* **1998**, *4*, 222.

(20) Speiser, B.; Würde, M.; Quintanilla, M. G. *Electrochem. Commun.* **2000**, *2*, 65.

(21) Weissensteiner, W.; Schuster, I. I.; Blount, J. F.; Mislow, K. *J. Am. Chem. Soc.* **1986**, *108*, 6664.

(22) Prinz, P.; Lansky, A.; Haumann, T.; Boese, R.; Noltemeyer, M.; Knieriem, B.; de Meijere, A. *Angew. Chem., Int. Ed. Engl.* **1997**, *36*, 1289.

(23) Dietrich, M.; Heinze, J.; Krieger, C.; Neugebauer, F. A. *J. Am. Chem. Soc.* **1996**, *118*, 5020.

(24) Poules, V. W.; Praefcke, K. *Chem. Zeit.* **1983**, *107*, 310.

(25) Testaferri, L.; Tingoli, M.; Tiecco, M. *J. Org. Chem.* **1980**, *45*, 4376.

(26) Testaferri, L.; Tiecco, M.; Tuigoli, M.; Chianelli, D.; Montanucci, M. *Synthesis* **1983**, 751.

(27) MacNicol, D. D.; Mallinson, P. R.; Murphy, A.; Sym, G. J. *Tetrahedron Lett.* **1982**, *23*, 4131.

(28) Garreau, D.; Savéant, J.-M. *J. Electroanal. Chem.* **1972**, *35*, 309.

(29) Frisch, M. J.; Trucks, G. W.; Schlegel, H. B.; Scuseria, G. E.; Robb, M. A.; Cheeseman, J. R.; Zakrzewski, V. G.; Montgomery, J. A., Jr.; Stratmann, R. E.; Burant, J. C.; Dapprich, S.; Millam, J. M.; Daniels, A. D.; Kudin, K. N.; Strain, M. C.; Farkas, O.; Tomasi, J.; Barone, V.; Cossi, M.; Cammi, R.; Mennucci, B.; Pomelli, C.; Adamo, C.; Clifford, S.; Ochterski, J.; Petersson, G. A.; Ayala, P. Y.; Cui, Q.; Morokuma, K.; Malick, D. K.; Rabuck, A. D.; Raghavachari, K.; Foresman, J. B.; Cioslowski, J.; Ortiz, J. V.; Stefanov, B. B.; Liu, G.; Liashenko, A.; Piskorz, P.; Komaromi, I.; Gomperts, R.; Martin, R. L.; Fox, D. J.; Keith, T.; Al-Laham, M. A.; Peng, C. Y.; Nanayakkara, A.; Gonzalez, C.; Challacombe, M.; Gill, P. M. W.; Johnson, B. G.; Chen, W.; Wong, M. W.; Andres, J. L.; Head-Gordon, M.; Replogle, E. S.; Pople, J. A. *Gaussian 98*, revision A.1; Gaussian, Inc.: Pittsburgh, PA, 1998.

(30) Titan 1.05; Wavefunction, Inc.; Schröninger, Inc.: Irvine, CA, 1999.

(31) Becke, A. D. *J. Chem. Phys.* **1993**, *98*, 5648.

(32) Hariharan, P. C.; Pople, J. A. *Chem. Phys. Lett.* **1972**, *16*, 217.

(33) (a) Hybrid density functional methods with the 6-31G* base have been used previously for calculations on neutral and radical cation of heterocycles containing sulphur atoms[33b−d] and on extended TTF and found to give a good qualitative description of properties. (b) Hernández, V.; Muguruma, H.; Hotta, S.; Casado, J.; López Navarrete, J. T. *J. Phys. Chem. A* **2000**, *104*, 735. (c) Keszthelyi, T.; Grage, M. M.-L.; Offersgaard, J. F.; Wilbrandt, R.; Svendsen, C.; Mortensen, O. S.; Pedersen, J. K.; Jensen, H. J. A. *J. Phys. Chem. A* **2000**, *104*, 2808. (d) Moore, A. J.; Bryce, M. R.; Batsanov, A. S.; Green, A.; Howard, J. A. K.; McKervey, A.; McGuigan, P.; Ledoux, I.; Orti, E.; Viruela, R.; Viruela, P. M.; Tarbit, B. *J. Mater. Chem.* **1998**, *8*, 1173.

(34) (a) Stewart, J. J. P. *J. Comput. Chem.* **1989**, *10*, 209. (b) Stewart, J. J. P. *J. Comput. Chem.* **1989**, *10*, 221.

(35) (a) Foresman, J. B.; Keith, T. A.; Wiberg, K. B.; Snoonian, J.; Frisch, M. J. *J. Phys. Chem.* **1996**, *100*, 16098. (b) For a general review about solvation methods, see: Cramer, J.; Truhlar, D. G. *Chem. Rev.* **1999**, *99*, 2161.

(36) For scan rates higher than 50 V s^{-1}, the variation of E_p with log v was not linear and larger than that obtained at smaller scan rates indicating that the overall electrochemical mechanism is more and more limited by the heterogeneous electron-transfer steps when decreasing the experimental time or increasing the scan rate.

(37) Andrieux, C. P.; Savéant, J.-M. Electrochemical Reactions. In *Investigations Of Rates and Mechanisms*; Bernasconi, C. F., Ed.; Wiley: New York, 1986; Vol. 6, 4/E, Part 2, pp 305−390.

(38) Andrieux, C. P.; Hapiot, P.; Savéant, J.-M. *Chem. Rev*. **1990**, *112*, 2439.

(39) Nadjo, L.; Savéant, J.-M. *J. Electroanal. Chem*. **1973**, *48*, 113.

(40) In such case, the influence of the solution electron-transfer (SET) $\mathbf{A} + \mathbf{B}^{\bullet -} \rightleftarrows \mathbf{A}^{\bullet -} + \mathbf{B}$ reaction is negligible.

(41) The ratio between the equilibrium constants corresponding to the chemical reaction steps at the level of the neutral ($K_{B/A}$) and radical anion forms ($K_{B^{\bullet -}/A^{\bullet -}}$) is directly related to the difference in the formal potentials ($E^{\circ\prime}_{A/A^{\bullet -}} - E^{\circ\prime}_{B/B^{\bullet -}}$) determined from high scan rate cyclic voltammograms.

(42) Nicholson, R. S.; Shain, I. *Anal. Chem*. **1964**, *36*, 706.

(43) Savéant, J.-M.; Vianello, E. *Electrochim. Acta* **1963**, *8*, 905.

(44) Alkylsulfonyl substituents S1 and S2 have different atomic environments because of the inversion of their closest neighbors (S2 and S4 for S1 and S3 and S5 for S6). It results that dihedral angles between the sulfonyl groups and the four central carbons on the ring are different and that S1 is non equivalent to S6.

(45) DFT calculations indicate an higher spin density in the vicinity of the S1 group, suggesting that this position is responsible for the ESR signal.

(46) We failed to obtained reliable optimized geometries for the bulkiest compounds (**1e** and **1d**) because many unsymmetrical conformers corresponding to local energy minimum were obtained depending on the starting geometry certainly because of very large energy barriers in this case.

(47) (a) Although data concerning the polar effect of different sulfonyl units are not available in the literature, it appears that the electron-donating character of the *iso*-propyl group is rather close to that of the linear alkyl chains, as shown by the values of the Taft polar substituent constants σ^*.[47b] (b) Taft, R. W., Jr. Separation of Polar, Steric, and Resonance Effects in Reactivity. In *Steric Effects in Organic Chemistry*; Newman, M. S., Ed.; Wiley & Sons: New York, 1956; pp 556−675.

(48) Contrary to the case of an electron-transfer concerted with the structural changes, the chemical step do not participate in the activation barrier.